2009 American Control Conference
Hyatt Regency Riverfront, St. Louis, MO, USA
June 10-12, 2009

Virtual sensors, application to vehicle tire-road normal forces for road safety

Moustapha Doumiati, Alessandro Victorino, Ali Charara and Daniel Lechner

Abstract— **The principal concerns in road safety are understanding and preventing risky situations. A close examination of accident data reveals that losing the vehicle control is responsible for a huge proportion of car accidents. Improving vehicle stabilization is possible when vehicle parameters are known. Unfortunately, some parameters like tire-road forces, which have a major impact on vehicle dynamics, are difficult to measure in a standard car. These data must therefore be observed or estimated. This study presents an estimation process for lateral load transfer and wheel-ground contact normal forces. The proposed method is based on the dynamic response of a vehicle instrumented with cheap, easy available standard sensors. The estimation process is composed of two parts: the main role of the first part is to estimate the oneside lateral load transfer, while in the second part we compare linear and nonlinear models for the estimation of vertical forces on the four wheels. Performances are tested using an experimental car in real driving situations. Experimental results show the potentiel of the estimation method.**

I. INTRODUCTION

Extensive research has shown that most of road accidents occur as a result of driver error [1]. Most drivers have little knowledge of dynamics, and so driver assistance systems have an important role to play. On-board ADAS (Advanced Driver Assistance Systems) control systems, require certain input data concerning vehicle states and vehicle-road interaction. Some of these dynamic states like longitudinal velocity, accelerations, yaw rate and suspension deflections are easily measured using low cost sensors (ABS speed sensor, accelerometers, gyrometers, ...). However, other essential parameters, such as tire-road forces that governed vehicle motion, are more difficult to measure because of technical, physical and economic reasons. These data must therefore be observed or estimated.

Knowledge of wheel-ground contact normal forces is essential for improving transport security. These forces have a primary influence on steering behavior, vehicle stability, cornering stiffness and lateral tire forces. Moreover, online measurement of vehicle tire forces in a moving vehicle allows a better calculation of the Lateral Transfer Ratio (LTR) parameter [2]. LTR is an indicator used to prevent or forecast rollover situations.

Estimating the vertical tire load is generally considered a difficult task. Variations in the vehicle's mass, the position of the center of gravity (cog), the road grade, road irregularities and the load transfer increase the complexity of the problem. In literature, several works have already been conducted in order to calculate vertical tire/road forces. In [3], the author presents a model for calculating vertical forces. Lechner's model respects the superposition principle, assuming independent longitudinal and lateral acceleration contributions. In [4], a study of a 14 DOF (Degree Of Freedom) vehicle model is proposed where the dynamics of the roll center are used to calculate vertical tire forces. In the work of [5], the tire forces are modeled by coupling longitudinal and lateral acceleration. Authors in [6] investigated the application of the DEKF (Dual Extended Kalman Filter) for estimating vertical forces. They concluded that the obtained results differ from the reference data, the discrepancy being attributable to the problem of the vehicle's mass.

The goal of this work is to develop a new real-time estimation process which use simple vehicle models and a certain number of valid measurements in order to estimate accurately the wheel-ground contact vertical forces. For simplicity reasons, vehicle models do not take into account pitch angle, road bank angle and irregularities.

The proposed estimation process is seperated in two parts that work in series. The first part estimates the one-side lateral load transfer by using roll dynamics. The estimated value will be considered as an essential measure for the second part, guaranteeing observers convergency and observability. The second part proposes and compares two observers for the four vertical tire forces estimation, and serves to calculate the LTR coefficient. Each part will be described in detail in the following sections. By using cascaded observers, the observability problems entailed by an inappropriate use of the complete modeling equations are avoided enabling the estimation process to be carried out in a simple and practical way.

The remainder of the paper is organized as follows. In sections 2 and 3, we describe in detail each of the observers designed for estimation of lateral load transfer and normal forces. Section 4 describes a method for identifying vehicle mass. Section 5 presents an observability analysis. Section 6 presents the estimation method. Section 7 introduces the importance of vertical forces for rollover calculations. In section 8, observers results are discussed and compared to real experimental data, and then in the final section we make some concluding remarks regarding our study and future perspectives.

II. PART I: LATERAL TRANSFER LOAD MODEL

The lateral load transfer model we have developed is based on the vehicle's roll dynamics. We use a roll plane model including the roll angle θ, as shown in figure 1. This model has a roll degree of freedom for the suspension that connects the sprung and unsprung mass, and its sprung mass is assumed to rotate about the roll center. During cornering, the roll angle depends on the roll stiffness of the axle and on the position of the roll center. In reality, the roll center of the vehicle does not remain constant, but in this study a stationary roll center is assumed in order to simplify the model.

M. Doumiati, A. Victorino and A. Charara are with Heudiasyc Laboratory, UMR CNRS 6599, Université de Technologie de Compiègne, 60205 Compiègne, France mdoumiat@hds.utc.fr, acorreav@hds.utc.fr and acharara@hds.utc.fr

D. Lechner is with Inrets-MA Laboratory, Departement of Accident Mechanism Analysis, Chemin de la Croix Blanche, 13300 Salon de Provence, France daniel.lechner@inrets.fr

978-1-4244-4524-0/09/$25.00 ©2009 AACC

According to the torque balance in the roll axis (the line which passes through the roll centers of the front and rear axles), the roll dynamics of the vehicle body can be described by the following differential equation (for small roll angle) [7]:

$$I_{xx}\ddot{\theta} + C_R\dot{\theta} + K_R\theta = m_s a_y h_{cr} + m_s h_{cr} g\theta, \qquad (1)$$

where I_{xx} is the moment of inertia of the sprung mass m_s with respect to the roll axis, C_R and K_R denote respectively the total damping and spring coefficients of the roll motion of the vehicle system and h_{cr} is the height of the sprung mass about the roll axis, and g is the gravitational constant. Summing the moments about the front and rear roll centers, the simplified steady-sate equation for the lateral load transfer applied to the left-hand side of the vehicle is given by the dynamic relationship (2) [8]:

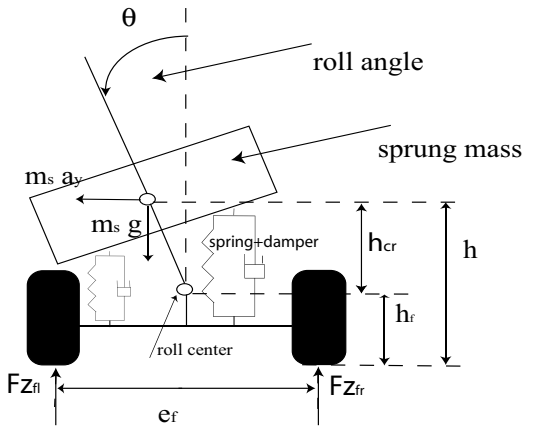

Fig. 1. Roll dynamics (front view)

$$\begin{aligned}\Delta Fz_l &= (Fz_{fl} + Fz_{rl}) - (Fz_{fr} - Fz_{rr}) \\ &= -2(\tfrac{k_f}{e_f} + \tfrac{k_r}{e_r})\theta - 2m_s\tfrac{a_y}{l}(\tfrac{l_r h_f}{e_f} + \tfrac{l_f h_r}{e_r})\end{aligned} \qquad (2)$$

where h is the height of the center of gravity (cog), h_f and h_r are the heights of the front and rear roll centers, e_f and e_r the vehicle's front and rear track, k_f and k_r the front and rear roll stiffnesses, l_r and l_f the distances from the cog to the front and rear axles respectively and l is the wheelbase ($l = l_r + l_f$) (see figure 2). We assume that the lateral load transfer applied to the right-hand ΔFz_r is equal to $-\Delta Fz_l$. The lateral acceleration a_y used in equations (1) and (2) is generated at the cog. The accelerometer, however, is unable to distinguish between the acceleration caused by the vehicle's motion on the one hand, and the gravitational acceleration on the other. In fact the acceleration a_{ym}, measured by the lateral accelerometer, is a combination of the gravitational force and the vehicle acceleration as represented in the following equation (for small roll angle):

$$a_{ym} = a_y + g\theta \qquad (3)$$

Measuring the roll angle requires additional sensors, which makes it a difficult and costly operation. In this study we consider that the roll angle can be calculated using relative suspension sensors. During cornering on a smooth road, the suspension is compressed on the outside and extended on the inside of the vehicle. If we neglect pitch dynamic effects on roll motion, the roll angle can be calculated by applying the following equation based on the geometry of the roll motion [7]:

$$\theta = \frac{(\delta_{fl} - \delta_{fr} + \delta_{rl} - \delta_{rr})}{(2e_f)} - \frac{m_v a_{ym} h}{k_t} \qquad (4)$$

where δ_{ij} (i represents the front(f) or the rear(r) and j represents the left(l) or the right (r)) is the suspension deflection (relative position of the wheel with respect to the vehicle body at each corner ij), k_t is the roll stiffness resulting from tire stiffness and m_v is the vehicle mass.

A. State-space representation-observer O_{1L}

By combining the relations (1), (2) (3) and (4), a linear state-space representation of the model described in the previous section can be given. The state vector X is:

$$X = \left[\Delta Fz_l\ \Delta Fz_r\ a_y\ \dot{a_y}\ \theta\ \dot{\theta}\right]. \qquad (5)$$

It is initialized as null vector. We assume that $\dot{a_y}$ is represented using a non-descriptive model ($\ddot{a_y} = 0$).
The observation vector Z is :

$$Z = \left[a_{ym}\ (\Delta Fz_l + \Delta Fz_r)\ \theta\ \dot{\theta}\ \Delta Fz_l\right] \qquad (6)$$

where,

- a_{ym}: lateral acceleration measured by the accelerometer;
- $\Delta Fz_l + \Delta Fz_r$: the sum of right and left transfer loads is assumed to be zero at each instant;
- θ: roll angle calculated using equation (4);
- $\dot{\theta}$: roll rate measured directly by the gyrometer;
- ΔFz_l: left transfer load calculated from equation (2).

Consequently, the state matrix A and the output matrix H are given as:

$$A = \begin{pmatrix} 0 & 0 & 0 & a_1 & 0 & a_2 \\ 0 & 0 & 0 & -a_1 & 0 & -a_2 \\ 0 & 0 & 0 & 1 & 0 & 0 \\ 0 & 0 & 0 & 0 & 0 & 0 \\ 0 & 0 & 0 & 0 & 0 & 1 \\ 0 & 0 & m_s\frac{h_{cr}}{I_{xx}} & 0 & \frac{m_s g h_{cr} - K_R}{I_{xx}} & \frac{-C_R}{I_{xx}} \end{pmatrix},$$

where:

$$\begin{aligned} a_1 &= -2\tfrac{m_s}{l}(\tfrac{l_r h_f}{e_f} + \tfrac{l_f h_r}{e_r}) \\ a_2 &= -2(\tfrac{k_f}{e_f} + \tfrac{k_r}{e_r}) \end{aligned} \qquad (7)$$

.

$$H = \begin{pmatrix} 0 & 0 & 1 & 0 & g & 0 \\ 1 & 1 & 0 & 0 & 0 & 0 \\ 0 & 0 & 0 & 0 & 1 & 0 \\ 0 & 0 & 0 & 0 & 0 & 1 \\ 1 & 0 & 0 & 0 & 0 & 0 \end{pmatrix}$$

The state vector $X(t)$ will be estimated by applying a Linear Kalman Filter (LKF) (see section VI).

III. Part II: Wheel ground vertical contact force model

As a result of longitudinal and lateral accelerations, the load distribution in a vehicle can significantly vary during movement. It can be expressed by the vertical forces that act on each of the four wheels. This section presents two models for calculating vertical forces. The first is a nonlinear model that takes into account longitudinal and lateral acceleration coupling, while the second applies the superposition assumption.

A. Nonlinear model

The force due to the longitudinal acceleration at the cog causes a pitch torque which increases the rear axle load and reduces the front axle load. In addition, during cornering the lateral acceleration causes a roll torque which increases the load on the outside and decreases it on the inside of the vehicle [5].
The load distribution can be expressed by the vertical forces that act on each of the four wheels (see figure 2). These equations are:

$$\begin{cases} Fz_{fl} = \frac{1}{2}m_v\left(\frac{l_r}{l}g - \frac{h}{l}a_x\right) - m_v\left(\frac{l_r}{l}g - \frac{h}{l}a_x\right)\frac{h}{e_f g}a_y \\ Fz_{fr} = \frac{1}{2}m_v\left(\frac{l_r}{l}g - \frac{h}{l}a_x\right) + m_v\left(\frac{l_r}{l}g - \frac{h}{l}a_x\right)\frac{h}{e_f g}a_y \\ Fz_{rl} = \frac{1}{2}m_v\left(\frac{l_f}{l}g + \frac{h}{l}a_x\right) - m_v\left(\frac{l_f}{l}g + \frac{h}{l}a_x\right)\frac{h}{e_r g}a_y \\ Fz_{rr} = \frac{1}{2}m_v\left(\frac{l_f}{l}g + \frac{h}{l}a_x\right) + m_v\left(\frac{l_f}{l}g + \frac{h}{l}a_x\right)\frac{h}{e_r g}a_y \end{cases} \quad (8)$$

where a_x is the longitudinal acceleration.

1) State-space representation-observer O_{2N}: Using relations (8) and the estimated results from the second block, a nonlinear state-space representation (nonlinear evolution model and linear observation model) of the system described in the section above can be given.
The vehicle state vector X is:

$$X = [Fz_{fl}\ Fz_{fr}\ Fz_{rl}\ Fz_{rr}\ a_x\ \dot{a}_x\ a_y\ \dot{a}_y]. \quad (9)$$

It is initialized as follows:

$$X_0 = [m_{fl}g\ m_{fr}g\ m_{rl}g\ m_{rr}g\ 0\ 0\ 0\ 0]. \quad (10)$$

where m_{ij} represents the quarter mass of the vehicle at each corner and is calculated as presented in section IV. The particular nonlinear function $f = (f_1, f_2, \ldots, f_8)$ representing the state equations is then given by:

$$\begin{cases} f_1 = \frac{-h}{2l}m_v x_6 - m_v\frac{l_r h}{le_f}x_8 + m_v\frac{h^2}{le_f g}x_5 x_8 \\ \quad +m_v\frac{h^2}{le_f g}x_6 x_7 \\ f_2 = \frac{-h}{2l}m_v x_6 + m_v\frac{l_r h}{le_f}x_8 - m_v\frac{h^2}{le_f g}x_5 x_8 \\ \quad -m_v\frac{h^2}{le_f g}x_6 x_7 \\ f_3 = \frac{h}{2l}m_v x_6 - m_v\frac{l_f h}{le_r}x_8 - m_v\frac{h^2}{le_r g}x_5 x_8 \\ \quad -m_v\frac{h^2}{le_r g}x_6 x_7 \\ f_4 = \frac{h}{2l}m_v x_6 + m_v\frac{l_f h}{le_r}x_8 + m_v\frac{h^2}{le_r g}x_5 x_8 \\ \quad +m_v\frac{h^2}{le_r g}x_6 x_7 \\ f_5 = x_6 \\ f_6 = 0 \\ f_7 = x_8 \\ f_8 = 0 \end{cases} \quad (11)$$

The measurement vector Z:

$$Z = \left[\Delta Fz_l\ (Fz_{fl} + Fz_{fr})\ a_x\ a_y\ \sum F_{ij}\right], \quad (12)$$

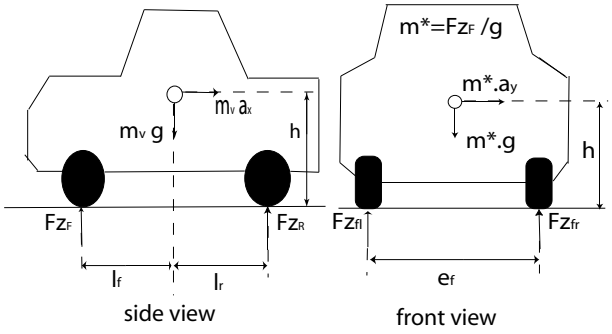

Fig. 2. *On the left side:* load shifting during acceleration; *on the right side:* wheel load shifting during cornering.

consists of the following components:

- ΔFz_l is provided by the observer O_{1L};
- $Fz_{fl} + Fz_{fr}$ is calculated directly from (8);
- a_x is measured using an accelerometer;
- a_y is provided by the the observer O_{1L};
- $\sum F_{ij}$ is assumed to be equal to $m_v g$ at each instant.

The observation function $h = (h_1,\ h_2, \ldots,\ h_5)$ takes the form:

$$\begin{cases} h_1 = x_1 - x_2 + x_3 - x_4 \\ h_2 = x_1 + x_2 \\ h_3 = x_5 \\ h_4 = x_7 \\ h_5 = x_1 + x_2 + x_3 + x_4 \end{cases} \quad (13)$$

The state vector $X(t)$ will be estimated by applying an Extended Kalman Filter (EKF) (see section VI).

B. Linear model

In this section a linear model that assumes the principle of superposition is used for calculating vertical forces [3]. The principle of superposition states that the total of a series of effects considered concurrently is identical to the sum of the individual effects considered individually. Therefore, we can numerically add the changes in wheel loads resulting from lateral and longitudinal load transfer in order to produce loads that are valid for combined operational conditions. The vertical forces are given as:

$$\begin{cases} Fz_{fl,fr} = m_v g\frac{l_r}{2l} - m_v\frac{h}{2l}a_x \pm m_v\frac{hl_r}{e_f l}a_y \\ Fz_{rl,rr} = m_v g\frac{l_f}{2l} + m_v\frac{h}{2l}a_x \pm m_v\frac{hl_f}{e_r l}a_y \end{cases} \quad (14)$$

1) State-space representation-observer O_{2L}: Considering equation (14) instead of equation (8), the system described in section III-A.1 becomes linear. The evolution and observation matrices, respectively A and H, are given as:

$$A = \begin{pmatrix} 0 & 0 & 0 & 0 & 0 & \frac{-m_v h}{2l} & 0 & \frac{-l_2 m_v h}{le_1} \\ 0 & 0 & 0 & 0 & 0 & \frac{-m_v h}{2l} & 0 & \frac{l_2 m_v h}{le_1} \\ 0 & 0 & 0 & 0 & 0 & \frac{m_v h}{2l} & 0 & \frac{-l_1 m_v h}{le_2} \\ 0 & 0 & 0 & 0 & 0 & \frac{m_v h}{2l} & 0 & \frac{l_1 m_v h}{le_2} \\ 0 & 0 & 0 & 0 & 0 & 1 & 0 & 0 \\ 0 & 0 & 0 & 0 & 0 & 0 & 0 & 0 \\ 0 & 0 & 0 & 0 & 0 & 0 & 0 & 1 \\ 0 & 0 & 0 & 0 & 0 & 0 & 0 & 0 \end{pmatrix},$$

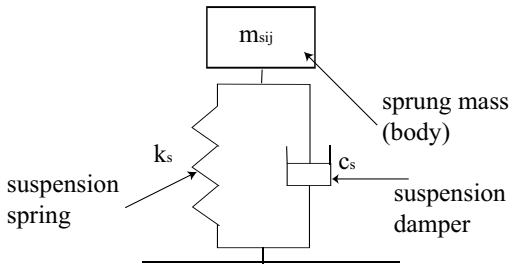

Fig. 3. Linear suspension of a quarter car-model neglecting tire dynamics.

$$H = \begin{pmatrix} 1 & -1 & 1 & -1 & 0 & 0 & 0 & 0 \\ 1 & 1 & 0 & 0 & 0 & 0 & 0 & 0 \\ 0 & 0 & 0 & 0 & 1 & 0 & 0 & 0 \\ 0 & 0 & 0 & 0 & 0 & 0 & 1 & 0 \\ 1 & 1 & 1 & 1 & 0 & 0 & 0 & 0 \end{pmatrix}$$

The state vector $X(t)$ will be estimated by applying the LKF.

IV. Determining the vehicle's mass

As described in sections II and III, the vehicle's mass m_v is an important parameter in studying lateral load transfer and vertical tire forces. Moreover, knowing the load distribution when the vehicle is at rest is essential for initializing the observers (III-A.1). This section deals with this problem and presents a method for determining a vehicle's mass.
Determining the mass of a vehicle is a problem seldom discussed in the literature. For example, in [9], a recursive least-squares method is developed for online estimation of a vehicle's mass. This method is unsuitable for our application because it takes a considerable time to converge to the real mass value. The objective of this section is to identify the vehicle's mass, by considering a quarter-car model, that neglects the tire deflection (figure 3), and applying relative position sensors. Nowadays, many controlled suspensions are equipped with relative position sensors for measuring suspension deflections δ_{ij}. The suspension spring is loaded with the corresponding sprung mass. The quarter mass m_{eij} (sum of the sprung and unsprung masses) at each corner of the empty vehicle is information provided by the manufacturer. Given a conventional suspension without level regulation, and assuming that it is functioning within its linear range, a load variation in the sprung mass Δm_{sij} changes the spring deflection $\delta_{ij} \rightarrow \delta_{ij} + \Delta ij$ where

$$\Delta m_{sij} = \frac{k_s \Delta_{ij}}{g}, \tag{15}$$

Δ_{ij} is the spring deflection variation, k_s the spring stiffness. The total quarter mass m_{ij} and the total mass of the vehicle m_v are then calculated as follows:

$$\begin{cases} m_{ij} &= m_{eij} + \Delta m_{sij} \\ m_v &= \sum_{i,j} m_{ij} \end{cases} \tag{16}$$

Then the static load (when the vehicle is at rest) applied to each wheel is equal to $m_{ij}g$. Experimental tests, that validate the presented identification method, are presented in section VIII-B (see figure 5).

V. Observability

Observability is a measure of how well the internal states of a system can be inferred from knowledge of its inputs and external outputs. This property is often presented as a rank condition on the observability matrix.

A. Linear system

The systems described in section II-A and III-B.1 are observable. For each system, we have verified that the system observability matrix O, defined in (17), has full rank:

$$O = \begin{bmatrix} H & HA & HA^2 & ... & HA^{n-1} \end{bmatrix} = n, \tag{17}$$

where n represents state-space vector dimension.

B. Nonlinear system

Using the nonlinear state space formulation of the system described in section III-A.1, the observability definition is local and uses the Lie derivative [10]. An observability analysis of this system was undertaken in [11]. It has been shown that the rank of the observability matrix during the experimental test corresponded to the state vector.

VI. Estimation methods

The aim of an observer or a virtual sensor is to estimate a particular unmeasurable variable from available measurements and a system model. This is an algorithm which describes the movement of the unmeasurable variable by means of statistical conclusions from the measured inputs and outputs of the system. A simple example of an open loop observer is the model given by relations (2), (4) and (8). Because of the system-model mismatch (unmodelled dynamics, parameter variations,...) and the presence of unknown, unmeasurable disturbances, the estimates obtained from the open loop observer would deviate from the actual values over time. In order to reduce the estimation error, at least some of the measured outputs are compared to the same variables estimated by the observer. The difference is fed back into the observer after being multiplied by a gain matrix K, and so we have a closed loop observer. All observers were implemented in a first-order Euler approximation discrete form. At each iteration, the state vector is first calculated according to the evolution equation and then corrected online with the measurement errors (innovation) and filter gain K in a recursive prediction-correction mechanism. The gain is calculated using the Kalman filter method [12], [13], where the process and measurement noise vectors are assumed to be white, zero mean and uncorrelated.

VII. Rollover avoidance

One important feature of the online calculation of vertical tire forces is rollover detection. This factor is recognized as one of the most significant life-threatening factors in car accidents. According to the statistics, nearly 33% of all deaths from passenger vehicle crashes result from rollovers. Several types of vehicle rollover propensity systems have been introduced, in order to predict this phenomenon on the basis of vehicle behavior. For instance, as a static roll stability indicator, the static stability factor (SSF), which is a ratio of the half track width to the height of vehicle's center of gravity, is commonly used to predict vehicle rollover. This factor is used as a static threshold for predicting rollover. To provide more realistic warnings, several dynamic approaches have been suggested including the time-to-rollover (TTR)

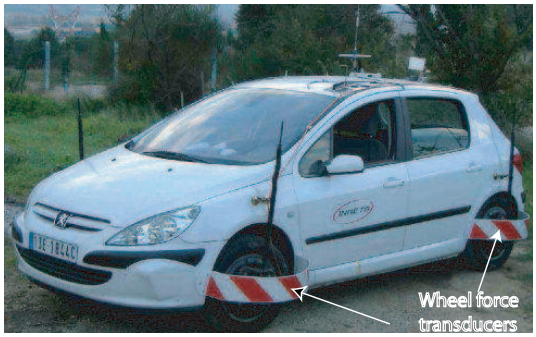

Fig. 4. Experimental vehicle

metric [14] and the lateral transfer ratio (LTR). The rollover index LTR, which is simply represented in equation (18), is suggested as a convenient method for supervising the vehicle's dynamic roll behavior [2],

$$LTR = \frac{Fz_l - Fz_r}{Fz_l + Fz_r} = \frac{\Delta Fz_l}{Fz_l + Fz_r}, \tag{18}$$

where Fz_l and Fz_r are respectively vertical loads on the left and right tires. The value of LTR varies from -1 at the lift-off of the left wheel, tends towards 0 at no load transfer, and to 1 at the lift-off of the right wheel. A simplified steady-state approximation of LTR in terms of lateral acceleration a_{ym} and the cog height h is given as [15]:

$$LTR = 2\frac{a_{ym}h}{ge_m}, \tag{19}$$

where a_{ym} is the lateral acceleration and e_m is the average track width ($e_m = (e_f + e_r)/2$). Rollover estimation based on equation (19), developed in steady-state situations, is not sufficient for detecting the rollover transient phase. The best way to identify the LTR is by estimating vertical forces. Subsequently, a direct precise measurement of the LTR can be used as a reliable rollover warning, or as a switch for a controller system [15].

VIII. Experimental results

A. Experimental car

The experimental vehicle shown in figure 4 is the INRETS-MA (Institut National de la Recherche sur les Transports et leur Sécurité - Département Mécanismes d'Accidents) Laboratory's test vehicle. It is a Peugeot 307 equipped with a number of sensors including accelerometers, gyrometers, steering angle sensors, linear relative suspension sensors, and Kistler wheel force transducers that currently cost in the region of 100.000 €, for a 6-components measurement system. These transducers measure in real time the forces and moments acting at the wheel center. The sampling frequency of the different sensors is 100Hz.

B. Validation of the vehicle's weight identification method

In order to validate the proposed method for determining the vehicle's weight (see section IV), two experimental tests were done. Five passengers were asked to sit in the car. Measurements (vertical forces and suspension deflections) were done with the car at rest, first with no passengers, then with one, with two, and so on. Then measurements were performed as the passengers left the car one by one until it was empty again. Disregarding suspension dynamics, we assume that real m_{ij} are equal to Fz_{ij}/g, where the Fz_{ij} are measured by the wheel force transducers. Figure 5 compares real m_{ij} with those that were the identified (see section IV). Although the identification method is simple, results overall are acceptable. However, some differences appear because of noise, model simplifications and the accuracy of the suspension deflection sensors. As described below, the identification method was applied in order to initialize observers (see section III).

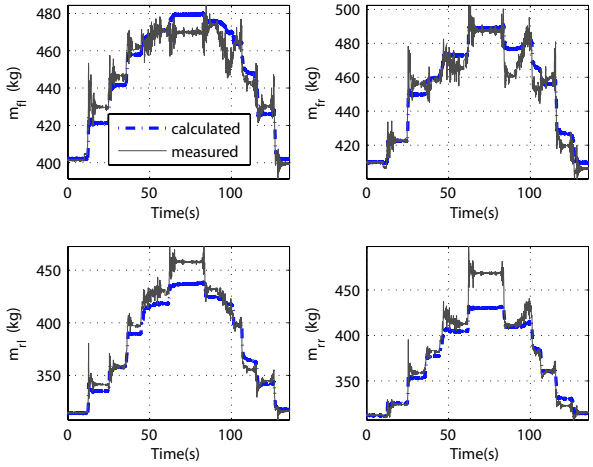

Fig. 5. Load distribution in terms of number of passengers

C. Test conditions

Test data from nominal as well as adverse driving conditions were used to assess the performance of the observers presented in sections II-A and III, in realistic driving situations. Among numerous experimental tests, we report lane-change manoeuvre where the dynamic contributions play an important role. Figure 6 presents the Peugeot's trajectory, its speed, steering angle and "g-g" acceleration diagram during the test. Acceleration diagrams show that large lateral accelerations were obtained (absolute value up to $0.6g$), meaning that the experimental vehicle was put in a critical driving situation.
The estimation process algorithm was written in C++ and has been integrated into the laboratory car as a DLL (Dynamic Link Library) that functions according to the software acquisition system.

D. Validation of observers

The observer results are presented in two forms: as tables of normalized errors, and as figures comparing the measurements and the estimations. The normalized error for an estimation z is defined as:

$$\epsilon_z = 100 \times \frac{\|z_{obs} - z_{measured}\|}{max(\|z_{measured}\|)} \tag{20}$$

where z_{obs} is the variable calculated by the observer, $z_{measured}$ is the measured variable and $max(\|z_{measured}\|)$ is the absolute maximum value of the measured variable during the test maneuver.

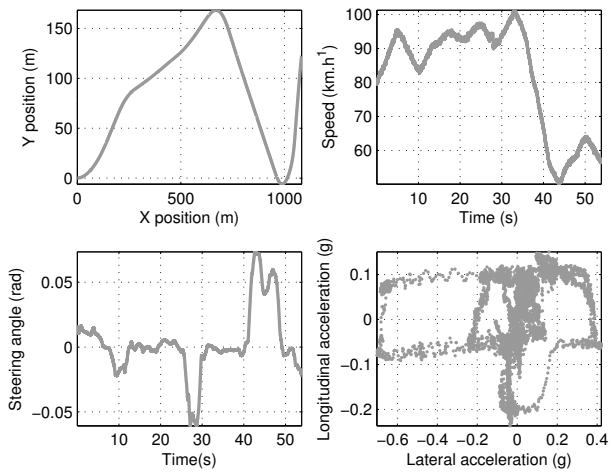

Fig. 6. Experimental test: vehicle trajectory, speed, steering angle and acceleration diagrams for the lane-change test

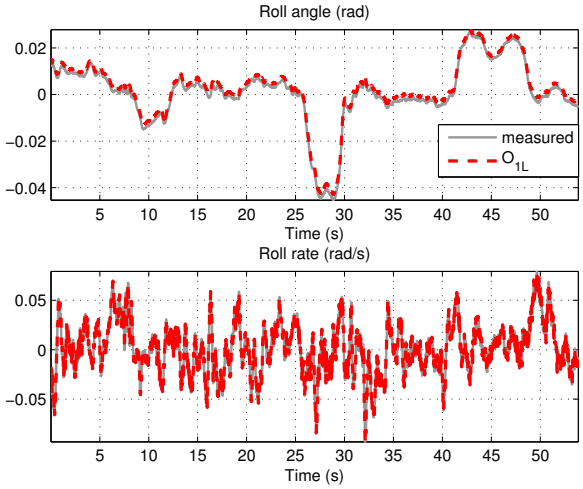

Fig. 7. Roll angle and roll rate.

Figure 7 presents the roll angle and the changes in the roll rate during the trajectory. Figure 8 shows the one-side lateral load transfer, while figure 9 and figure 10 show vertical forces on the front and rear wheels. These figures show that the observers are highly accurate with respect to measurements. Some small differences during the trajectory are to be noted. These might be explained by neglected geometrical parameters such as camber angle. Tables I and II present maximum absolute values, normalized mean errors and normalized std for lateral transfer load, roll angle, vertical forces and the LTR parameter. We can deduce that for this test the performance of the observer is satisfactory, with normalized error globaly less than 5%.

Finally, figure 11 compares the LTR obtained from measured forces, estimated forces and the calculated LTR according to equation (19). We deduce that the estimated LTR fits the measured LTR well. Moreover, it is clear that the calculated LTR is not able to give a good approximation in the transient phase. Online calculation of the LTR is

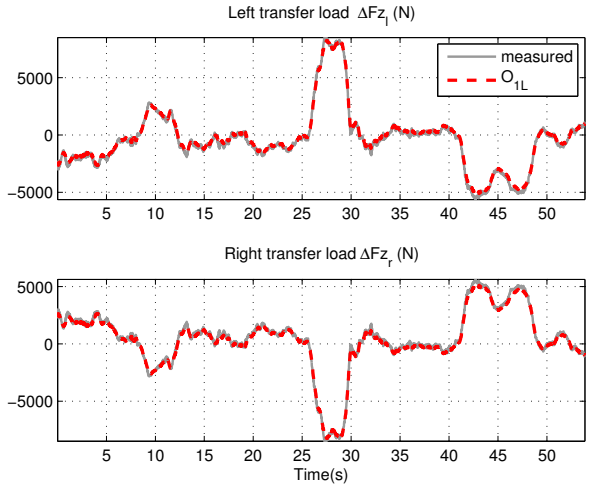

Fig. 8. Lateral transfer load.

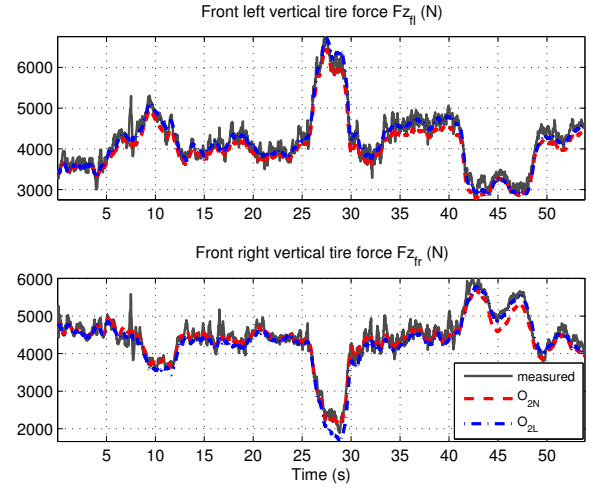

Fig. 9. Estimation of front vertical tire forces.

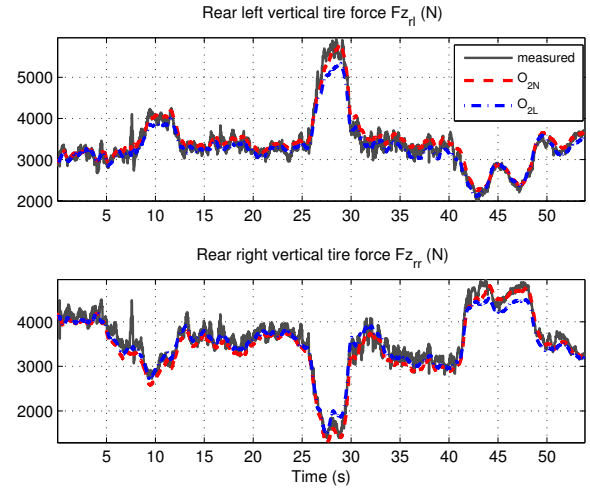

Fig. 10. Estimation of rear vertical tire forces.

	Max $\|\|\|$	Mean %	Std %
ΔFz_l	5635 (N)	2.83	2.15
θ	0.026 (rad)	5.5	0.83

TABLE I

OBSERVER O_{1L}: MAXIMUM ABSOLUTE VALUES, NORMALIZED MEAN ERRORS AND NORMALIZED STD.

O_{2N} \ O_{2L}	Max $\|\|\|$	Mean %	Std %
Fz_{fl}	6755 (N)	2.9 / 2.83	1.92 / 1.9
Fz_{fr}	6008 (N)	2.8 / 2.5	2.36 / 1.93
Fz_{rl}	5958 (N)	2.23 / 2.15	2.14 / 1.66
Fz_{rr}	4948 (N)	3.01 / 3.25	2.27 / 2.37
LTR	0.48	1.74 / 1.73	1.34 / 1.33

TABLE II

OBSERVERS O_{2N} AND O_{2L}: MAXIMUM ABSOLUTE VALUES, NORMALIZED MEAN ERRORS AND NORMALIZED STD.

essential for rollover avoidance; when LTR exceeds a set value, the driver must be alerted in order to prevent a dangerous situation, or an automatic control system must be activated in order to avoid rollover.

Comparing O_{2L} and O_{2N} observers, we find that O_{2N} is more efficient, especially during the time interval [25s-30s]. This can be explained by the fact that during this time, heavy demands are made on the vehicle, and the longitudinal/lateral coupling dynamics become more significant than the superposition principle. Consequently, observer O_{2N} proves able to work better than O_{2L}.

IX. CONCLUSION

This paper has presented a new algorithm to estimate lateral transfer load and vertical tire forces, regardless of the tire model. Our study presents three observers (O_{1L}, O_{2L} and O_{2N}) developed for this purpose and based on the Kalman filter. Observer O_{1L} is based on a roll dynamics model and provides lateral load transfer estimation. Observers O_{2L} and O_{2N} are derived respectively from linear and nonlinear models. The linear model rests on the longitudinal and lateral dynamics superposition principle, while the nonlinear model proposes coupling these dynamics. The LTR rollover index parameter was also calculated and discussed within the context of estimating vertical wheel forces.

Experimental evaluations in real-time embedded estimation processes yield good estimations close to the measurements. However, we note that the observer O_{2N} gives better results when high longitudinal/lateral accelerations act simultaneously.

The potential of the estimation process demonstrates that it may be possible to replace expensive dynamometric hub sensors by software observers that can work in real-time while the vehicle is in motion. This is one of the important results of our work.

Although the identified mass tends toward the real mass value, one of the weak points of this approach is the determination of the vehicle's mass, which is highly dependent on the sensitivity of the relative suspension sensors. Moreover, the suspension model is considered linear, which does not always correspond to reality.

Future studies will improve the vehicle mass identification method, and take into account road irregularities and road bank angle, which can significantly impact load transfer. Moreover, the effect of normal tire load on the estimation of lateral forces will be studied.

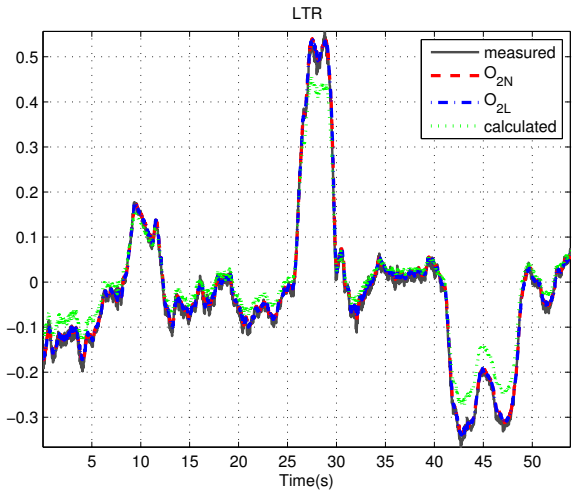

Fig. 11. Estimation of the LTR parameter.

REFERENCES

[1] F. Aparicio et al, *Discussion of a new adaptive speed control system incorporating the geometric characteristics of the road*, Int. J. Vehicle Autonomous Systems, vol.3, No.1, pp.47-64, 2005.

[2] F. Boettiger, K. Hunt and R. Kamnik, *Roll dynamics and lateral load transfer estimation in articulated heavy freight vehicles*, Proc.Instn Mech. Engrs Vol. 217 Part D: J. Automobile Engineering, 2003.

[3] D. Lechner, *Analyse du comportement dynamique des vehicules routiers légers: développement d'une méthodologie appliquée à la sécurité primaire*, Ph. D, dissertation Ecole Centrale de Lyon, France, 2002.

[4] T. Shim and C. Ghike, *Understanding the limitations of different vehicle models for roll dynamics studies*, Vehicle System Dynamics, volume 45, pages 191-216, March 2007.

[5] U. Kiencke and L. Nielsen, *Automotive control systems*, Springer, 2000.

[6] T.A. Wenzel et al, *Dual extended Kalman filter for vehicle state and parameter estimation*, Vehicle System Dynamics, volume 44, pages 153-171, February 2006.

[7] T. Brown, A. Hac and J. Martens, *Detection of vehicle rollover*, SAE World Congress, Michigan-Detroit, March 2004.

[8] W.F. Milliken and D.L. Milliken, *Race car vehicle dynamics*, Society of Automotive Engineers, Inc, U.S.A, 1995.

[9] A. Vahidi, A. Stefanopoulou and H. Peng, *Recursive least squares with forgetting for online estimation of vehicle mass and road grade: theory and experiments*, Vehicle System Dynamics, volume 43, pages 31-55, January 2005.

[10] H. Nijmeijer and A.J. Van der Schaft, *Nonlinear dynamical control systems*, Springer Verlag, 1991.

[11] M. Doumiati, A. Victorino, A. Charara, D. Lechner and G. Baffet, *An estimation process for vehicle wheel-ground contact normal forces*, IFAC WC'08, Seoul Korea, july 2008.

[12] R.E. Kalman, *A new approach to linear filtering and prediction problems*, Transactions of the ASME- Journal of Basic Engineering. vol. 82. series D. pp.35-45,1960.

[13] G. Welch and G. Bishop, *An introduction to the Kalman Filter*, Course 8, University of North Carolina, chapel Hill, Departement of computer science, 2001.

[14] C. B. Chen and H. Peng, *A Real-time rollover threat index for sports utility vehicles*. Proc. of the American Control Conference, 1999.

[15] D. Ödenthal, T. Bunte and J. Ackerman, *Nonlinear steering and breaking control for vehicle rollover avoidance*, European control conference, 1999.